Scalable synthesis of djurleite copper sulphide (Cu1.94S) hexagonal nanoplates from a single precursor copper thiocyanate and their photothermal properties

ARTICLE *in* CRYSTENGCOMM · MAY 2015

Impact Factor: 4.03 · DOI: 10.1039/C5CE00638D

9 AUTHORS, INCLUDING:

Donghwan Yoon
Korea University
10 PUBLICATIONS **18** CITATIONS
SEE PROFILE

Suhyun Park
Korea University
6 PUBLICATIONS **10** CITATIONS
SEE PROFILE

Hionsuck Baik
Korea University
44 PUBLICATIONS **299** CITATIONS
SEE PROFILE

Seungjoo Haam
Yonsei University
202 PUBLICATIONS **3,822** CITATIONS
SEE PROFILE

CrystEngComm

COMMUNICATION

View Article Online
View Journal | View Issue

Cite this: *CrystEngComm*, 2015, **17**, 4627

Received 31st March 2015,
Accepted 13th May 2015

DOI: 10.1039/c5ce00638d

www.rsc.org/crystengcomm

Scalable synthesis of djurleite copper sulphide ($Cu_{1.94}S$) hexagonal nanoplates from a single precursor copper thiocyanate and their photothermal properties†

Donghwan Yoon,[a] Haneul Jin,[a] Suho Ryu,[b] Suhyun Park,[a] Hionsuck Baik,[c] Seung Jae Oh,[d] Seungjoo Haam,[e] Chulmin Joo*[b] and Kwangyeol Lee*[a]

Copper sulphide materials have received great attention due to their low bandgap semiconducting properties. As compared to other chalcogenides, few synthetic examples have been reported, and a simple and scalable synthetic method for preparing size- and shape-controlled copper sulphide nanoparticles is required for potential wide application of these materials. Herein, a facile one pot scalable synthetic route has been developed for preparing highly monodisperse djurleite $Cu_{1.94}S$ hexagonal nanoplates. The thermal decomposition of a single precursor CuSCN was found suitable for preparing a large quantity of highly monodisperse $Cu_{1.94}S$ hexagonal nanoplates; a multi-gram scale product could be obtained in a single step. Under the synthetic scheme developed, the width of $Cu_{1.94}S$ nanoplates with a thickness of ~ 10 nm could be easily tuned from 70 nm to 130 nm. Their optical properties were investigated and their photothermal effect was also studied by photothermal optical coherence reflectometry (PT OCR). $Cu_{1.94}S$ hexagonal nanoplates showed a considerable photothermal effect, which was found to depend on the nanoparticle concentration.

Semiconductor nanoparticles have received great attention due to their potential application in various fields such as absorbers in solar cells,[1–5] bio-application,[6–10] sensors,[11–13] and laser sources.[14–16] Copper sulphides with their low energy bandgaps have been extensively investigated for photovoltaic application, and can be classified into three groups according to the Cu/S ratio: monosulphides ($1.6 \leq Cu/S \leq 2$), mixed monosulphide and disulphide ($1.0 \leq Cu/S \leq 1.6$), and disulphides (CuS_2).[17] In particular, monosulphides, namely, $Cu_{1.94}S$ (djurleite), $Cu_{1.8}S$ (digenite), $Cu_{1.75}S$ (anilite) and $Cu_{1.6}S$ (geerite), have received great attention due to their semiconducting properties. Therefore, there is a strong demand for a reliable and scalable synthetic route to this important class of nanoparticles for practical applications. However, scalable synthetic routes to highly monodisperse copper sulphide nanoparticles with a well-defined shape and composition are very rare, due to the difficulty in controlling the Cu/S stoichiometry. We envisaged that the decomposition of a single precursor with a preformed Cu–S bond might provide us a better control over the stoichiometry of the resulting copper sulphide phase. Therefore, we attempted to decompose a single precursor CuSCN, which is commercially available, to form monodisperse and composition-controlled copper sulphide nanoparticles. Herein, we report an efficient synthetic method to synthesize size-controlled $Cu_{1.94}S$ hexagonal nanoplates in large quantities as well as their well-defined optical properties.

In a typical synthesis of $Cu_{1.94}S$ hexagonal nanoplates, a slurry of CuSCN in oleylamine was prepared in a 100 mL Schlenk tube. After placing the reaction mixture under vacuum at 100 °C for 10 min, the reaction mixture was charged with 1 atm Ar gas. Then the Schlenk tube was placed in a hot oil bath, which was preheated to 240 °C. After heating at the same temperature for 30 min, the reaction mixture was cooled down to room temperature, washed several times with toluene and methanol, followed by centrifugal separation to give $Cu_{1.94}S$ hexagonal nanoplates. This one pot synthetic method is very scalable and several grams of nanoparticles could be easily obtained without sacrificing the structural uniformity (see Fig. S1† for the picture of the product obtained from 12 grams of CuSCN).

Representative TEM images and FFT patterns of $Cu_{1.94}S$ hexagonal nanoplates are shown in Fig. 1 and S2.† The

[a] *Department of Chemistry and Research Institute for Natural Science, Korea University, Seoul 136-701, Korea. E-mail: kylee1@korea.ac.kr; Tel: +82 2 3290 3139*
[b] *School of Mechanical Engineering, Yonsei University, Seoul 120-749, Korea. E-mail: cjoo@yonsei.ac.kr*
[c] *Korea Basic Science Institute (KBSI), Seoul 136-713, Korea*
[d] *Medical Convergence Research Institute, College of Medicine, Yonsei University, Seoul, Korea*
[e] *Department of Chemical and Biomolecular Engineering, College of Engineering, Yonsei University, Seoul 120-749, Korea*

† Electronic supplementary information (ESI) available. See DOI: 10.1039/c5ce00638d

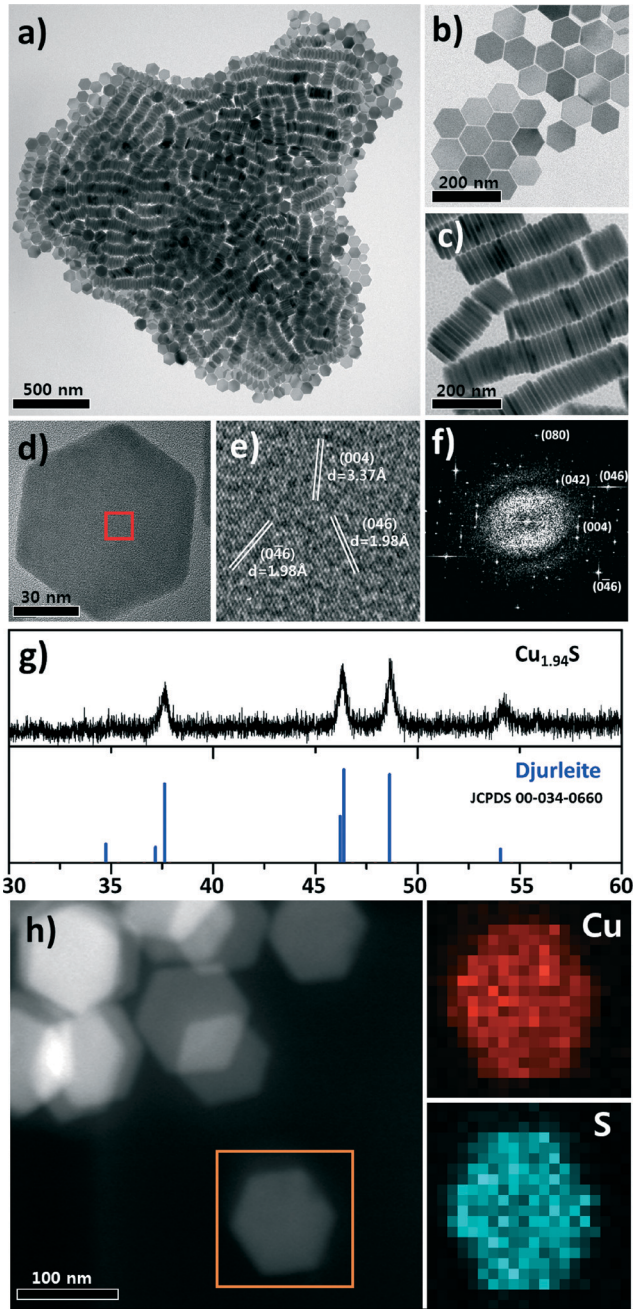

Fig. 1 TEM and HRTEM images of $Cu_{1.94}S$ hexagonal nanoplates. a) TEM image at low magnification. b) Planar nanoplates viewed from above. c) Stacked nanoplates. d–f) HRTEM image and corresponding FFT pattern with zone axis ($\bar{1}00$). g) XRD pattern of $Cu_{1.94}S$ nanocrystals. h) STEM images and energy dispersive X-ray spectroscopy analysis of $Cu_{1.94}S$ hexagonal nanoplates prepared on a nickel grid. Elemental mapping data shows 66.34% Cu and 33.65% S.

nanoparticles shown in Fig. 1a–c are highly uniform with an average size of 86.1 ± 2.9 nm and a thickness of 10.7 ± 1.3 nm. The nanocrystal size was defined as the diagonal point to point distance. In most experimental results, the values of standard deviation (σ) were under 5% of the average size, indicating the uniformity of the nanoplate size. The nanoplates can be assembled by either face-to-face stacking or edge sharing as shown in Fig. 1b–c. During synthesis, we used oleylamine as solvent and surfactant, and the distance between stacked nanoplates is about 1.28 nm, which corresponds to the interdigitated oleylamine bilayer thickness (see ESI† Fig. S3). Similar stacking of nanoplates has also been reported for other nanoparticles with monodisperse sizes and homogeneous shapes.[18,19]

The crystal structure of $Cu_{1.94}S$ is quite complex as shown in the FFT images in Fig. 1f. The structure is consistent with the previously reported monoclinic system, with space group $P2_1/n$, a = 26.897 Å, b = 15.745 Å, c = 13.565 Å, and β = 90.13°. 31 sulphur atoms and 62 copper atoms are found in one unit cell.[20] In order to solve the structural complexity, the FFT pattern was simulated and analysed by combining the X-ray diffraction pattern and the computer simulated one using JEMS software (see Fig. S4† for detailed simulation results). Previously, $Cu_{1.94}S$ was sometimes wrongly assigned as Cu_2S due to the high similarity of their XRD patterns.[21] In our case, a ratio of 1.94 was identified by careful analysis of the XRD pattern and computer simulation of the TEM diffraction pattern using an image simulation software program. Fig. 1h displays the high-angle annular dark-field scanning TEM (HAADF-STEM) image of the $Cu_{1.94}S$ hexagonal nanoplates and the energy-dispersive X-ray (EDX) spectra measured from a single nanoplate. The elemental mapping data shows Cu and S atom distributions in the hexagonal nanoplate; the ratio of 66.34% Cu and 33.65% S atoms is very similar to the Cu/S ratio of the $Cu_{1.94}S$ phase (see ESI† Fig. S5 for elemental analysis). X-ray photoelectron spectroscopy (XPS) analysis was carried out to obtain further information about the chemical composition of the nanoparticle surface (see ESI† Fig. S6). The Cu/S ratio was calculated from the peak area of the Cu and S peaks and was found to be 2.14, which is slightly higher than the value from EDX analysis. This high Cu content might be attributed to the binding of oleylamine ligands to the surface-exposed Cu atoms. The stability of $Cu_{1.94}S$ nanocrystals is well documented, and the Cu_2S phase is easily transformed to the $Cu_{1.94}S$ phase when exposed to air.[22] The heat of formation (enthalpy) ΔH_f of Cu_xS was calculated by Wei's group,[23] and the stabilities of Cu_xS including the monoclinic, hexagonal, cubic, and orthorhombic system were compared in terms of their ΔH_f. Djurleite $Cu_{1.94}S$ crystallizes in the monoclinic system with ΔH_f = −0.40 eV and low-chalcocite Cu_2S also belongs to the monoclinic system with ΔH_f = −0.41 eV. This indicates that $Cu_{1.94}S$ is more stable than low-chalcocite Cu_2S even under Cu-rich conditions and that Cu vacancies can be generated easily in Cu_2S.[24]

The size of the nanoplates could be efficiently modulated by changing the precursor concentration from 1 mM to 50 mM (ESI† Fig. S7) and the reaction temperature from 180 °C to 280 °C, as shown in Fig. 2. Under the reaction conditions employed, the size of the nanocrystals varies from about 70 nm to 126 nm. We observed that the growth of the nanoplates becomes very slow after a reaction time of 20 min (see ESI† Fig. S8), and the nanoparticle shape does not deteriorate by prolonged heating up to 1 h at a reaction temperature of

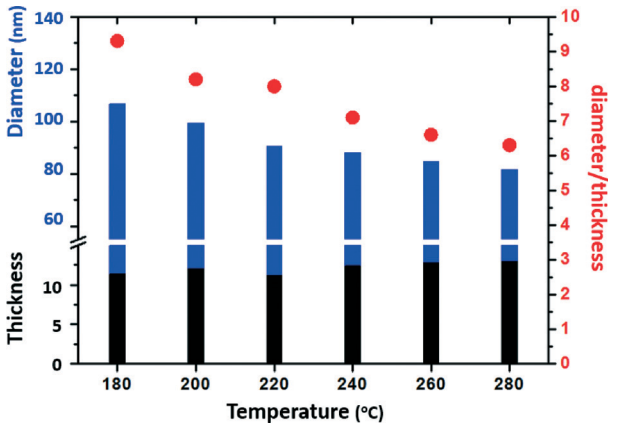

Fig. 2 Nanoplate size control depending on reaction temperature. The height of the black bar represents the thickness and the combined height of the black bar and blue bar represents the nanoparticle width. The aspect ratio change depending on synthetic temperature is also shown as red dots, which should be read according to the scale shown on the right.

240 °C. At reaction temperatures below 180 °C, the nanoparticle formation is so slow that the precursor could not be consumed completely; therefore reaction temperatures lower than 180 °C are not suitable for the formation of hexagonal nanoplates of $Cu_{1.94}S$. The average size increases with increased precursor concentration and decreases with higher reaction temperature. It is likely that the nucleation is much facilitated at higher temperatures, resulting in overall nanoparticle size decrease. It is notable that the nanoparticle size increases with increased precursor concentration. This seems to point to the fact that the number of nanoparticle seeds is rather similar, regardless of the precursor concentration, at the same temperature. Interestingly, the aspect ratio (size/thickness) of the nanoplates decreases with increased reaction temperature. This indicates the existence of a preferred growth direction of the nanoplates, along the width direction, at low reaction temperature. The synthesis of other nanostructures by using $Cu_{1.94}S$ nanoparticles as a template has been previously reported.[25–28] Thus, the size- and shape-controlled $Cu_{1.94}S$ nanocrystals from this study might serve as useful synthetic platforms for other important nanomaterials.

The optical absorption spectrum of the $Cu_{1.94}S$ nanoplates in Fig. 3a shows a broad range of absorbance from the UV to infrared (IR) region. The wide-range absorption of $Cu_{1.94}S$ is suitable for application as a solar cell absorber. The absorption spectra of $Cu_{1.94}S$ show an increased absorption in the near-IR region due to the interband transition from valence states to unoccupied states, which is similar to the finding with CuS nanoparticles.[29–32] The photoluminescence spectrum of $Cu_{1.94}S$ in Fig. 3a inset shows luminescence peaks at 405, 427 and 450 nm which originated from the direct band gap transition, similar to a previous report.[33] Most of the reported copper sulphide nanoparticles have two absorption peaks which are due to a direct bandgap in the UV region and an indirect bandgap in the NIR region; however it is still

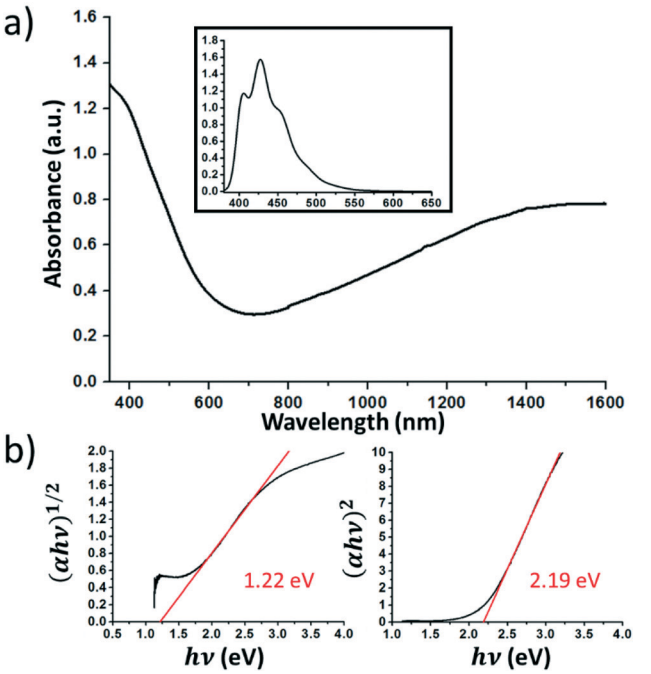

Fig. 3 a) Absorbance of 88.1 nm $Cu_{1.94}S$ hexagonal nanoplates and photoluminescence spectra (inset). PL spectrum was taken at 350 nm excitation. b) Plot of $(\alpha h\nu)^{1/2}$ *vs.* $h\nu$ for assessment of indirect bandgap and $(\alpha h\nu)^2$ *vs.* $h\nu$ for assessment of direct bandgap.

controversial.[21] The optical bandgap E_g and the corresponding absorption coefficient α near the absorption edge show a relationship as shown below.[34]

$$\alpha h\nu = C(h\nu - E_g)^k$$

where C is a constant and $h\nu$ is the photon energy; the value of k is 0.5 for an indirect bandgap and 2 for a direct bandgap. Thus, the optical bandgap could be estimated by extrapolating the fitting line of the plot, namely, the Tauc plot. As shown in Fig. 3b, the optical bandgaps are estimated to be 1.22 eV and 2.19 eV for the indirect and direct optical bandgaps, respectively, of the synthesized $Cu_{1.94}S$ hexagonal nanoplates. The direct bandgap value from the Tauc plot is rather different from the experimental blue-shifted photoluminescence value, which might be attributed to the quantum confinement effect of thin $Cu_{1.94}S$ nanoplates.[29]

Recently, a photothermal effect of copper sulphide nanocrystals, which might be useful for tumoricidal effects, in the near IR region was reported.[35–38] It is very important to develop biodegradable photothermal agents for future theranostic applications.[39] Au nanoparticles, while being useful for photothermal applications, are not biodegradable. In order to understand the photothermal response of the $Cu_{1.94}S$ nanoplates prepared in this work, we examined the optical phase changes ($\Delta\phi$) of the 840 nm probe light reflected from a quartz cuvette filled with aqueous nanoparticle solution (see Fig. S9 and S10† for detailed experimental scheme). We measured the phase of the interference between

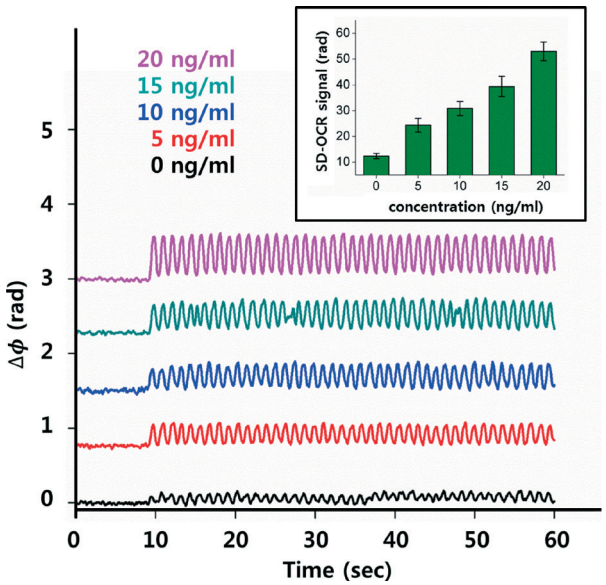

Fig. 4 PT responses of $Cu_{1.94}S$ hexagonal nanoplates. The measured phase signal at different $Cu_{1.94}S$ concentrations. The intensity of the PT excitation light source was 6 W cm^{-2}. (Inset) PT responses of the $Cu_{1.94}S$ nanoparticles *vs.* $Cu_{1.94}S$ concentrations. The PT responses varied linearly with the $Cu_{1.94}S$ concentrations. The error bar denotes the standard error based on 10 measurements.

the reflections from the top and bottom surfaces of the inner chamber. Upon irradiation with 1064 nm photothermal (PT) excitation light, the nanoparticles absorbed the PT light energy, generating heat. This thermal change leads to an alteration of the optical phase difference between the top and bottom surfaces of the chamber. Fig. 4 shows the phase signal measured with our setup for 60 seconds under 6 W cm^{-2} PT light illumination. The PT excitation light source was modulated at 1 Hz modulation. The measured phase of the $Cu_{1.94}S$ nanoplate solution varied markedly under the PT excitation, whereas the nanoparticle-free solution exhibited a small phase change due to the intrinsic absorption of toluene at ~1064 nm. The measured PT responses at different nanoparticle concentrations are shown in the inset of Fig. 4. It can be seen that the measured PT response varies linearly with the concentration of the nanoplate solution. These results suggest the possibility of using these nanoparticles as powerful photothermal therapeutic agents.

Conclusions

In summary, we developed a scalable synthetic methodology for preparing $Cu_{1.94}S$ hexagonal nanoplates with a highly uniform size distribution from the thermal decomposition of a single precursor CuSCN in oleylamine. The size of the nanoplates could be conveniently controlled by simple variation of reaction temperature and precursor concentration. The $Cu_{1.94}S$ nanocrystals show absorption signals in a wide range from UV to NIR and optical phase changes, applicable to photothermal therapy. Further extension of the synthetic methodology to other metal systems and biological application of photothermal $Cu_{1.94}S$ nanoplates are currently under way.

Acknowledgements

This work was supported by the BioNano Health-Guard Research Center funded by the Ministry of Science, ICT & Future Planning (MSIP) of Korea as a Global Frontier Project (grant number H-GUARD_ 2013M3A6B2078946), NRF (20100020209), and MIHWAF (project: HI10C1911).

Notes and references

1 I. Gur, N. A. Fromer, M. L. Geier and A. P. Alivisatos, *Science*, 2005, **310**, 462–465.
2 A. Kongkanand, K. Tvrdy, K. Takechi, M. Kuno and P. V. Kamat, *J. Am. Chem. Soc.*, 2008, **130**, 4007–4015.
3 E. H. Sargent, *Nat. Photonics*, 2012, **6**, 133–135.
4 A. Cho, S. Ahn, J. H. Yun, J. Gwak, H. Song and K. Yoon, *J. Mater. Chem.*, 2012, **22**, 17893–17899.
5 J. Tang, Z. Huo, S. Brittman, H. Gao and P. Yang, *Nat. Nanotechnol.*, 2011, **6**, 568–572.
6 M. Bruchez Jr., M. Moronne, P. Gin, S. Weiss and A. P. Alivisatos, *Science*, 1998, **281**, 2013–2016.
7 B. Dubertret, P. Skourides, D. J. Norris, V. Noireaux, A. G. Brivanlou and A. Libchaber, *Science*, 2002, **298**, 1759–1762.
8 S. Kim, Y. T. Lim, E. G. Soltesz, A. M. D. Grand, J. Lee, A. Nakayama, J. A. Parker, T. Mihaljevic, R. G. Laurence, D. M. Dor, L. H. Cohn, M. G. Bawendi and J. V. Frangioni, *Nat. Biotechnol.*, 2004, **22**, 93–97.
9 S. Goel, F. Chen and W. Cai, *Small*, 2014, **4**, 631–645.
10 Z. Zha, S. Zhang, Z. Deng, Y. Li, C. Li and Z. Dai, *Chem. Commun.*, 2013, **49**, 3455–3457.
11 L. Shi, V. D. Paoli, N. Rosenzweig and Z. Rosenzweig, *J. Am. Chem. Soc.*, 2006, **128**, 10378–10379.
12 P. T. Snee, R. C. Somers, G. Nair, H. P. Zimmer, M. G. Bawendi and D. G. Nocera, *J. Am. Chem. Soc.*, 2006, **128**, 13320–13321.
13 R. C. Somer, M. G. Bawendi and D. G. Nocera, *Chem. Soc. Rev.*, 2007, **36**, 579–591.
14 H.-J. Eisler, V. C. Sundar, M. G. Bawendi, M. Walsh, H. I. Smith and V. Klimov, *Appl. Phys. Lett.*, 2002, **80**, 4614.
15 P. T. Snee, Y. Chan, D. G. Nocera and M. G. Bawendi, *Adv. Mater.*, 2005, **17**, 1131–1136.
16 V. I. Klimov, A. A. Mikhailovsky, S. Xu, A. Malko, J. A. Hollingsworth, C. A. Leatherdale, H.-J. Eisler and M. G. Bawendi, *Science*, 2000, **290**, 314.
17 L. S. Whiteside and R. J. Goble, *Can. Mineral.*, 1986, **24**, 247–258.
18 F. Huang, J. Zhou, J. Xu and Y. Wang, *CrystEngComm*, 2014, **16**, 9478.
19 J. Paek, C. H. Lee, J. Choi, S.-Y. Choi, A. Kim, J. W. Lee and K. Lee, *Cryst. Growth Des.*, 2007, **7**, 1378.
20 H. T. Evans Jr, *Science*, 1979, **203**, 26.
21 Y. Zhao and C. Burda, *Energy Environ. Sci.*, 2012, **5**, 5564–5576.

22 Y. Wu, C. Wadia, W. Ma, B. Sadtler and A. P. Alivisatos, *Nano Lett.*, 2008, **8**, 2551–2555.
23 Q. Xu, B. Huang, Y. Zhao, Y. Yan, R. Noufi and S.-H. Wei, *Appl. Phys. Lett.*, 2012, **100**, 061906.
24 M. Loftipour, T. Machani, D. P. Rossi and K. E. Plass, *Chem. Mater.*, 2011, **23**, 3032–3038.
25 J. E. Macdonald, M. B. Sadan, L. Houben, I. Popov and U. Banin, *Nat. Mater.*, 2010, **9**, 810–815.
26 K.-H. Park, Y. W. Lee, D. Kim, K. Lee, S. B. Lee and S. W. Han, *Chem. – Eur. J.*, 2012, **18**, 5874–5878.
27 J. Kolny-Olesiak, *CrystEngComm*, 2014, **16**, 9381–9390.
28 K. Vinokurov, Y. Bekenstein, V. Gutkin, I. Popov, O. Millo and U. Banin, *CrystEngComm*, 2014, **16**, 9506–9512.
29 M. Tanveer, C. Cao, Z. Ali, I. Aslam, F. Idrees, W. S. Khan, F. K. But, M. Tahir and N. Mahmood, *CrystEngComm*, 2014, **16**, 5290.
30 M. Tanveer, C. Cao, I. Aslam, Z. Ali, F. Idrees, M. Tahir, W. S. Khan, F. K. But and A. Mahmood, *RSC Adv.*, 2014, **4**, 63447.
31 P. Zhang and L. Gao, *J. Mater. Chem.*, 2003, **13**, 2007.
32 J. Gao, Q. Li, H. Zhao, L. Li, C. Liu, Q. Gong and L. Qi, *Chem. Mater.*, 2008, **20**, 6263.
33 M. D. Regulacio, C. Ye, S. H. Lim, M. Bosman, L. Polavarapu, W. L. Koh, J. Zhang, Q.-H. Xu and M.-Y. Han, *J. Am. Chem. Soc.*, 2011, **133**, 2052.
34 J. Tauc, *Mater. Res. Bull.*, 1968, **3**, 37.
35 B. Li, Q. Wang, R. Zhoum, X. Liu, K. Xu, W. Li and J. Hu, *Nanoscale*, 2014, **6**, 3274–3282.
36 S. W. Hsu, K. On and A. R. Tao, *J. Am. Chem. Soc.*, 2011, **133**, 19072–19075.
37 J. M. Luther, P. K. Jain, T. Ewers and A. P. Alivisatos, *Nat. Mater.*, 2011, **11**, 361–366.
38 Q. Tian, M. Tang, Y. Sun, R. Zou, Z. Chen, M. Zhu, S. Yang, J. Wang, J. Wang and J. Hu, *Adv. Mater.*, 2011, **23**, 3542–3547.
39 E.-K. Lim, T. Kim, S. Paik, S. Haam, Y.-M. Huh and K. Lee, *Chem. Rev.*, 2015, **115**, 327–394.